DYNAMIC RESPONSE OF AXIALLY CONSTRAINED PLASTIC BEAMS TO BLAST LOADS

R. VAZIRI,† M. D. OLSON‡ and D. L. ANDERSON‡

Department of Civil Engineering, University of British Columbia, Vancouver, B.C.,
Canada

Abstract—The analysis of a rigid, perfectly plastic rectangular beam with constrained ends subjected to a rectangular pressure pulse of finite duration is presented. Closed form expressions are obtained for the maximum permanent deflection for both simply supported and clamped boundary conditions. These expressions are valid for the full dynamic range from pseudo-static step load to high pressure impulsive loading. The results indicate that the response is strongly influenced by geometry changes even for small deflections. Finally the response expressions are combined to form isoresponse relationships which when plotted form isoresponse curves of direct engineering use.

NOTATION

$F(1\sqrt{2}, \phi)$	incomplete elliptic integral of the first kind with modulus $1/\sqrt{2}$ and amplitude ϕ
I	impulse in pressure pulse per unit length, $P_m\tau$
I_0	ideal impulse, eqn (39)
K	complete elliptic integral of the first kind with modulus $1/\sqrt{2}$
L	half-beam length
M	bending moment
M_0	fully plastic bending moment
N	axial force
N_0	fully plastic axial force
$P(t)$	pressure load per unit length
P_m	intensity of rectangular pulse
P_0	static collapse pressure per unit length
Q	shear force
T	time at which travelling hinges arrive at midspan
V_0	amplitude of velocity profile
b	beam width
c	wave speed, $\sqrt{(N_0/m)}$
cn	Jacobian elliptic function
h	beam depth
m	mass per unit length of beam
p	nondimensional pressure, P_m/P_0
p_c	limiting nondimensional pressure for long load duration
sd	Jacobian elliptic function
t	time
t_f	response duration
t_s	time at which string mode starts
w	transverse deflection
w_0	transverse central deflection
x	coordinate measured from centre of undeformed beam axis
β	nondimensional impulse parameter, I^2/mhP_0
β_0	impulsive limit of β, I_0^2/mhP_0
β_c	step load limit of β corresponding to p_c
$\dot{\epsilon}$	extensional strain rate
μ	dimensionless time scale, eqns (49a, b)
μ_c	limiting value of μ, eqns (50a, b)
$\rho(t)$	plastic hinge position at time t, Fig. 1(c)
τ	pulse duration
ϕ	amplitude of elliptic integral F, eqn (15)
ψ	curvature rate
$(\,\dot{}\,), (\,)'$	$\dfrac{\partial}{\partial t}(\,), \dfrac{\partial}{\partial x}(\,)$.

---

† Graduate student.

‡ Professors, Department of Civil Engineering, University of British Columbia, Vancouver, B.C., Canada V6T 1W5.

1. INTRODUCTION

The behaviour of structures under transient dynamic loads sufficiently strong to cause large permanent deformation is a subject of considerable interest, and has a wide variety of practical applications.

The general field of dynamic plastic analysis of structures is broad and the published literature is very extensive; a number of survey articles have appeared during the last few years[1–5]. The most recent compilation and analysis of published research results on air-blast reponse of beams and plates was presented by Ari-Gur et al.[6]. Among the numerous articles in the field of dynamic plasticity only a few will be mentioned, with emphasis on those which give theoretical analyses of beams.

The rigid-plastic idealization has been used by most authors. In one of the earliest works in this field, Lee and Symonds[7] treated the problem of a transverse impact force applied at the midpoint of a uniform beam with free ends. In a subsequent paper[8] Symonds obtained simple solutions for clamped and simply supported beams subjected to uniformly distributed loading with time histories that satisfied the restricted definition of the so-called "blast type" loading (i.e. loads that instantaneously rise to a peak magnitude and then mono-tonically decrease). Symonds and Mentel[9] studied the influence of axial restraints on the behaviour of rigid-plastic beams loaded with a uniformly distributed transverse impulse. Humphreys[10] conducted a series of experimental tests on flat steel beams using sheet ex-plosives to provide a short duration impulsive type loading. It was then concluded that for engineering purposes the rigid-plastic solution including axial constraints gave a fairly good approximation of the permanent plastic damage due to impulsive loading. Nonaka[11] made a theoretical and experimental investigation into the response of a clamped, axially restrained beam with a concentrated mass at its centre subjected to impact loading.

Jones[12] suggested a simple method for estimating the combined influence of strain-hardening and strain-rate sensitivity on the permanent deformation of impulsively loaded rigid-plastic beams. Jones[13] also investigated the behaviour of rigid-plastic rectangular beams subjected to uniform "dynamic" step loads of finite durations, using an approximate theoretical procedure which included the influence of finite deflections. This approximate procedure utilized time-independent deformation profiles identical to the corresponding static collapse ones. However, above a certain magnitude of the pressure pulse, the deformed shapes are expected to be time dependent. Krajcinovic[14] derived a closed form solution for the dynamic infinitesimal response of a simply supported rigid-plastic beam subjected to a uniformly distributed dynamic load of arbitrary pressure–time history.

A number of references on numerical analysis of elastoplastic structures have been cited in the review articles[1–6]. These methods may be needed for more general problems but remain expensive and rather time consuming.

It is clear from a survey of the literature that there are very few "exact" rigid-plastic solutions of beams which retain the influence of finite deflections and also account for the time distribution of the dynamic loading. In particular, the problem of a simple beam with constrained ends subject to a blast-type load of arbitrary duration has not previously been solved in closed form.

In the present paper, the analysis of a rigid-perfectly plastic rectangular beam with constrained ends subjected to a pressure pulse of finite duration is presented. The defor-mation proceeds under two distinct mechanisms depending on the level of the peak pressure. These mechanisms are described by kinematically admissible velocity fields that satisfy the appropriate continuity conditions. Although the governing equations are derived for a general pressure–time relationship, they are only solved for the particular case of a rec-tangular pulse. It is assumed that the latter forms a limiting case of a blast-type loading. Closed form expressions are developed for the prediction of the maximum permanent deflection. Finally the dependence of the permanent deflection on the applied pressure and impulse is obtained for a family of rectangular pulses. The results are represented by isoresponse curves in a form convenient for direct engineering use.

This paper constitutes a brief outline of the research work reported in [15], and fuller details may be found therein.

2. FORMULATION AND ANALYSIS OF THE PROBLEM

2.1. *Assumptions*

In the following analysis, the material of the beam is considered rigid, perfectly plastic and strain-rate insensitive. The dynamic pressure pulse $P(t)$ which acts uniformly over the entire beam length, is assumed to be of rectangular shape with intensity P_m and duration τ. Although finite deflections are taken into account, their magnitudes are considered to be small enough (compared to the beam length) so that the axial force can be taken as constant along the beam. Following the linear theory of Symonds[8] and Krajcinovic[14], the initial motion of the beam is assumed to proceed under two different mechanisms according to whether the load intensity is "low", $P_0 < P_m < 3P_0$ or "high", $P_m > 3P_0$, where P_0 is the static collapse load.

A detailed analysis is presented for the case of a simply supported beam of uniform rectangular cross-section. The results for the corresponding clamped ends case are also summarized.

2.2. *General description of response*

In the initial part of the motion, the deflected shape of the beam consists of a single central hinge with two rigid connecting pieces [Fig. 1(b)] if the pressure is low enough. For higher pressures, the deflected shape is more complicated, with hinges forming away from the centre [Fig. 1(c)] but moving towards the centre as motion proceeds. These two cases will be referred to as beam mechanism 1 and beam mechanism 2, respectively. The equations of motion for these two cases are nonlinear.
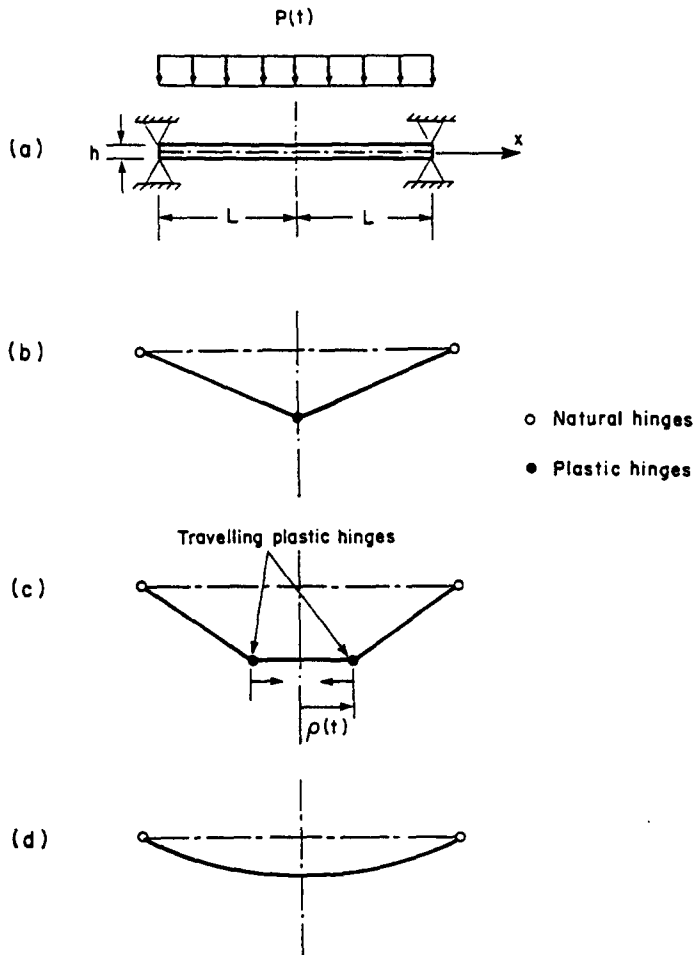

Fig. 1. Beam nomenclature and mechanisms of deformation.

As the motion proceeds and the deflections increase, the axial load increases and moment resistance decreases until at a central deflection of $h/2$ (the half-depth), the entire section is in tensile yield and the beam can no longer resist moments. At this point the beam acts as a string with a constant tension and the governing equation of motion is linear. We call this the string mode [Fig. 1(d)].

In the process of performing the analysis there are many cases that have to be considered, and one of the most difficult problems is keeping track of where you are in the solution process. Figure 2(a) shows a flow chart of the solutions that must be considered for the case of low pressure pulses. With reference to the figure, the initial motion of the structure is that of a loaded beam that has both bending and axial restraint. This is indicated in the figure with a heavy vertical line marked LBM1 (Loaded Beam Mechanism 1). This motion continues until one of three things occur:

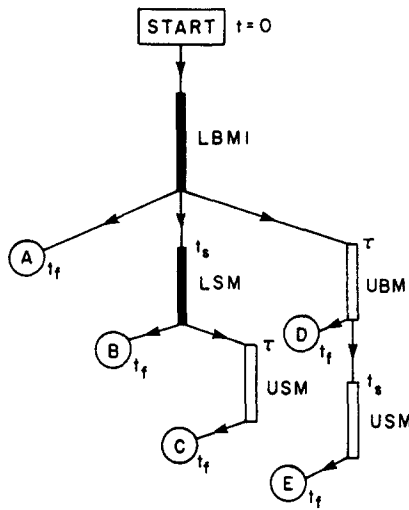(i) The beam comes to rest. This is indicated by the circled letter A and t_f, i.e. final time.

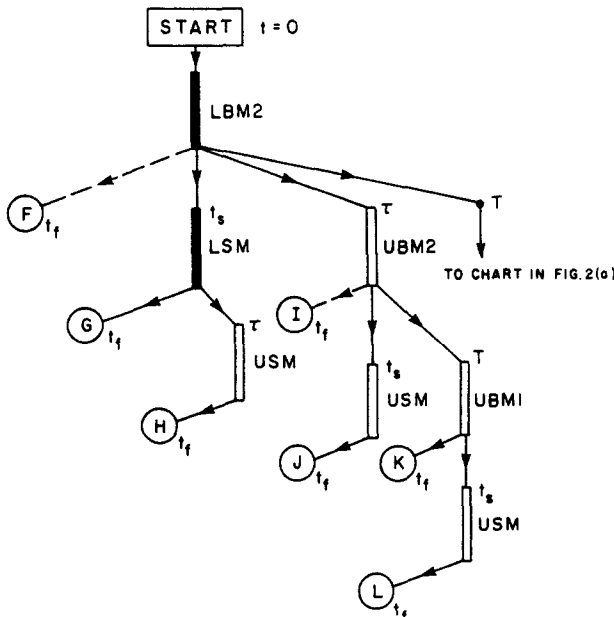
Fig. 2(a). Flow chart of solution branches for low load.

Fig. 2(b). Flow chart of solution branches for high load.

(ii) The beam deflection reaches $h/2$, at which point the bending resistance is zero and the member responds as a string. This is marked with t_s, i.e. string time.

(iii) The time reaches the pulse duration τ, and the load is removed.

The first case (A) is a terminal situation, and will result in permanent deformations less than $h/2$.

For motion beyond t_s, the structure responds as a string with the load still applied. Thus a heavy vertical line labelled LSM (Loaded String Mode) is drawn down from that point. Now this motion proceeds until the member comes to rest (B) or the end of the pulse is reached (τ) at which time any further response would be as an unloaded string, marked USM. The unloaded string motion then continues until the member comes to rest (C).

Returning to the original motion, if the third situation occurred, i.e. τ is reached before t_f or t_s, then the subsequent motion would be as an unloaded beam, marked UBM1. Following this line down could lead to the member coming to rest (D), or the deflection increasing until the string stage t_s is reached, at which point the unloaded string (USM) equations would govern until the motion ceased (E).

For higher pressures, the initial deflected shape has two symmetrically located hinges moving in towards the centre [Fig. 1(c)]. This is called Beam Mechanism 2 (BM2) and Fig. 2(b) shows the flow chart for the solution steps for this case. When and if the hinges reach the centre, the subsequent motion continues on with one hinge which is then the same solution as used for the low pressure beam, i.e. LBM1 or UBM1. In this figure, T represents the case where the hinges reach the centre before the t_f, t_s or τ conditions are reached. The other new term is UBM2 which stands for the unloaded beam mechanism 2 response. The dotted lines to points (F and I) represent conditions which one may think possible, but because of the requirements for the double-hinged mechanism cannot occur. Note that the string mode can be reached directly by the beam mechanism 2 response.

From Figs 2(a) and (b), it is seen that there are three basic types of response, the beam with a central hinge, the double hinged beam with moving hinges and the plastic string. In each type there is also the loaded and unloaded cases, which although not changing the solution form requires matching of conditions at the time of going from the loaded to unloaded stages.

The beam and string equations and solutions will be presented in general. However, the detailed analysis of all the possible solution branches will not be given, only the expressions for the final permanent deflections and guidelines on the pressure and impulse parameters that lead to each particular branch.

2.3. *Equation of motion, yield condition and associated flow rule*

Let x be the coordinate measured from the centre of the undeformed beam's centroidal axis, w, the transverse deflection, M and Q, the bending moment and shear force, respectively, N, the axial force and m, the mass per unit length of the beam. By D'Alembert's principle, the inertia load is $-m\ddot{w}(x, t)$ and the equation of motion of the beam can be written as

$$N(t)w''(x, t) + M''(x, t) = Q'(x, t) = m\ddot{w}(x, t) - P(t). \tag{1}$$

The yield condition which specifies the critical combination of axial load and bending moment under which plastic flow can occur for a rectangular cross-section is

$$\frac{M}{M_0} + \left(\frac{N}{N_0}\right)^2 = 1 \tag{2}$$

where M_0 and N_0 are the fully plastic values of bending moment and axial load, respectively. Also $4M_0/N_0 = h$, where h denotes the beam depth.

The flow rule appropriate to the above yield condition has been shown by Onat and

Prager[16] to take the form

$$\frac{N_0 \dot{\varepsilon}}{M_0 \dot{\psi}} = 2\frac{N}{N_0} \tag{3}$$

where $\dot{\varepsilon}$ is the extensional strain rate and $\dot{\psi}$ the curvature rate of the centroidal axis. Figure 3 illustrates, in geometrical terms, the parabolic yield curve [eqn (2)] and its associated flow law. For the deformation mechanisms of Figs 1(b) and (c), it is a simple matter to show that the ratio of the strain rates $\dot{\varepsilon}/\dot{\psi} = w_0$, so that the flow rule as expressed by eqn (3) becomes

$$\frac{N}{N_0} = \frac{N_0 w_0}{2M_0} = \frac{2w_0}{h} \tag{4}$$

where $w_0 = w(0, t)$ is the central deflection. Thus as long as $w_0 < h/2$, $N < N_0$ and eqns (2) and (3) hold. Once w_0 reaches $h/2$, $N = N_0$ and the moment resistance is reduced to zero, and the beam behaves as a string under constant tension. We will first consider the dynamic behaviour of the beam under small deformations $(w_0 \leqslant h/2)$ and subsequently treat the plastic string response at large deflections $(w_0 \geqslant h/2)$.

2.4. Beam mechanism 1: $P_0 < P_m < 3P_0$

The geometry of mechanism 1 suggests a linear velocity profile of the form

$$\dot{w}(x, t) = \dot{w}_0(t)\left[1 - \frac{x}{L}\right] \quad \text{for} \quad 0 \leqslant x \leqslant L \tag{5}$$

where L is the half-length of the beam. The initial conditions here are $w_0(0) = \dot{w}_0(0) = 0$. It may be shown that the configuration of mechanism 1 leads to a violation of the plasticity condition [eqn (2)] as the axial load builds up. However, owing to its mathematical simplicity this mechanism might reasonably be taken as a first approximation during small but finite deflections. The equation for dynamic equilibrium of the beam in terms of the axial load and moment at the centre is then

$$Nw_0 + M = \frac{L^2}{2}[P(t) - \tfrac{2}{3}m\ddot{w}_0]. \tag{6}$$
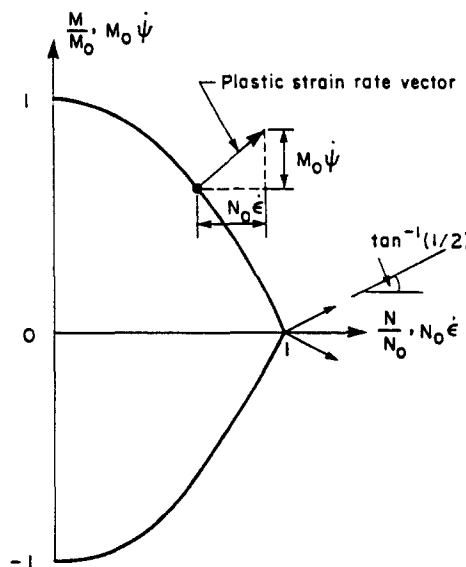
Fig. 3. Parabolic yield surface and plastic flow vector.

Using the yield condition and the flow rule, eqns (2) and (4), respectively, leads to

$$M_0 \left[1 + \frac{4}{h^2} w_0^2 \right] = \frac{L^2}{2} [P(t) - \tfrac{2}{3} m \ddot{w}_0].$$ (7)

(i) *Loaded phase, LBM*1. For a rectangular pressure pulse with $P(t) = P_m$, eqn (7) can be simplified to

$$\ddot{w}_0 + \lambda w_0^2 = v$$ (8)

where

$$\lambda = \frac{6P_0}{mh^2}$$ (9)

and

$$v = \frac{3}{2m} (P_m - P_0)$$ (10)

with $P_0 = 2M_0/L^2$ for a simply supported beam. The solution of eqn (8) can be obtained by multiplying each side by $2\dot{w}_0$ and integrating, which yields

$$\dot{w}_0^2 + \frac{2\lambda}{3} w_0^3 - 2v w_0 = \text{constant}$$ (11)

where the constant of integration vanishes here due to the initial conditions. Separation of variables followed by an integration of eqn (11) leads to

$$t = \sqrt{(\alpha/v)} \int_\phi^{\pi/2} \frac{d\phi}{\sqrt{(1 - \tfrac{1}{2} \sin^2 \phi)}}$$ (12)

where

$$\alpha^2 = \frac{3v}{\lambda} = \tfrac{3}{4} h^2 (p-1); \qquad 0 < \alpha \leqslant \sqrt{(3/2)} h$$ (13)

and

$$p = P_m/P_0$$ (14)

$$\phi = \cos^{-1} \sqrt{(w_0/\alpha)}.$$ (15)

The integral in eqn (12) can be evaluated explicitly, so that

$$t = \sqrt{(\alpha/v)} [K(1/\sqrt{2}) - F(1/\sqrt{2}, \phi)]$$ (16)

where $K = K(1/\sqrt{2}) \approx 1.854$, is the complete elliptic integral of the first kind with modulus $1/\sqrt{2}$, and $F(1/\sqrt{2}, \phi)$ is the incomplete elliptic integral of the first kind with modulus $1/\sqrt{2}$ and amplitude ϕ. Equation (16) yields the time t required to reach a specific deflection $w_0(t)$. Upon regrouping the terms, eqn (16) becomes

$$F(1/\sqrt{2}, \phi) = K - at$$ (17)

where

$$a = \sqrt{(\nu/\alpha)} = \sqrt{(P_0/mh)}\,[3(p-1)]^{1/4}. \tag{18}$$

From eqns (15) and (17), it follows that

$$w_0(t) = \alpha \cos^2 \phi = \alpha \; cn^2(K-at) \tag{19}$$

where *cn* is a Jacobian elliptic function.

The motion of the beam in this phase continues until one of the following three situations occurs:

(a) the beam comes to rest at $t = t_f$,
(b) the transition from beam to string behaviour occurs at $t = t_s$, or
(c) the load is suddenly removed at $t = \tau$ and the unloaded phase commences.

Case (a) represents a terminal situation with permanent deformation of the beam. The time t_f at which the beam comes to rest can be determined from eqn (19) as $t_f = K/a$. The final deflection is then given by $w_0(t_f) = \delta_f$, or in nondimensional form

$$\frac{\delta_f}{h} = \frac{\sqrt{3}}{2}\,[p-1]^{1/2}. \tag{20}$$

It can be shown that for $\delta_f/h \leqslant 1/2$, the pressure ratio $p \leqslant 4/3$. If $p > 4/3$, the beam will not cease moving in this phase and the string mode may be reached before the load comes off at $t = \tau$. With the aid of eqns (15) and (17), the time t_s at which the string mode starts is given by $t_s = (1/a)\,[K - F(1/\sqrt{2}, \phi_s)]$, where

$$\phi_s = \cos^{-1}(\sqrt{(h/2\alpha)}) = \cos^{-1}\left[\frac{1}{3(p-1)}\right]^{1/2}. \tag{21}$$

Furthermore, the central velocity at this instant can be obtained from eqn (11) by setting $w_0 = h/2$. The string mode analysis is given in Section 2.6.

(ii) *Unloaded phase, UBM*1. During this phase of motion, the beam is unloaded and continues to move until:

(a) the deformation finishes at $t = t_f$, or
(b) the central deflection w_0 reaches $h/2$ at $t = t_s$.

Following the same procedure as developed earlier, the governing equation of motion [eqn (11)] reduces to

$$\dot{w}_0^2(t) + \frac{2\lambda}{3} w_0^3(t) + \frac{3}{m} P_0 w_0(t) = \frac{3}{m} P_m w_0(\tau) \tag{22}$$

where $w_0(\tau) = \alpha \; cn^2(K - a\tau)$ is the central displacement at the termination of the loaded phase, which provides the initial conditions for this phase.

In case (a) above, the final central deflection δ_f can readily be obtained from eqn (22) by setting $\dot{w}_0(t_f) = 0$. Thus, in nondimensional form we have

$$\frac{\delta_f}{h} + \frac{4}{3}\left(\frac{\delta_f}{h}\right)^3 = \frac{\sqrt{3}}{4} p\sqrt{(p-1)}\,sd^2\{\sqrt{\beta}\,[3(p-1)]^{1/4}/p\} \tag{23}$$

where sd is a Jacobian elliptic function and

$$\beta = \frac{I^2}{mhP_0} \tag{24}$$

where

$$I = \int_0^\tau P(t)\, dt = P_m \tau \tag{25}$$

is the total impulse (per unit length) applied to the beam.

In case (b) above, the string stage is reached before the deformation finishes, and the initial velocity of the string must match that of the beam at $t = t_s$ given by eqn (22) with $w_0(t_s) = h/2$.

2.5. Beam mechanism 2: $P_m > 3P_0$

The velocity field for mechanism 2 [Fig. 1(c)] is given by

$$\dot{w}(x, t) = \begin{cases} \dot{w}_p(t), & \text{for} \quad 0 \leqslant x \leqslant \rho(t) \\ \dot{w}_p(t)\dfrac{L-x}{L-\rho(t)}, & \text{for} \quad \rho(t) \leqslant x \leqslant L \end{cases} \tag{26}$$

where $w_\rho(t)$ is the deflection and $\rho(t)$ the distance from the beam centre of the travelling hinge point. Owing to the symmetry of the problem we refer only to the right half of the beam in the following.

Differentiating eqn (26) with respect to time yields

$$\ddot{w}(x, t) = \begin{cases} \ddot{w}_\rho(t), & \text{for} \quad 0 \leqslant x \leqslant \rho(t) \\ [\ddot{w}_p(t) + \dot{\rho}\dot{w}_p(t)/(L-\rho)]\dfrac{L-x}{L-\rho(t)}, & \text{for} \quad \rho(t) \leqslant x \leqslant L \end{cases} \tag{27}$$

as the acceleration field. Within the flat central region confined by the hinges, the moment is constant and hence the shear is zero. Therefore, it follows from eqn (1) that the equation of motion for the central flat segment is

$$m\ddot{w}_p = P(t) \tag{28}$$

with initial conditions $w_\rho(0) = \dot{w}_\rho(0) = 0$.

The equation of motion for the outer segment of the beam is similar to that of the single hinge mechanism [Fig. 1(b)] of the previous analysis. Assuming that all the deformation consisting of both bending and stretching occurs in the outer segment of the beam, eqn (11) can be made to apply in this case merely by replacing L, w_0 and $\ddot{w}_0$ by $L-\rho$, w_p and $\ddot{w}_p + \dot{\rho}\dot{w}_p/[L-\rho]$, respectively. As a result, the equation of motion for the outer segment becomes

$$M_0\left(1 + \frac{4}{h^2}w_\rho^2\right) = \tfrac{1}{6}(L-\rho)^2 P(t) - \tfrac{1}{3}m\dot{w}_p\dot{\rho}(L-\rho) \tag{29}$$

where eqn (28) has been used to eliminate the acceleration term $\ddot{w}_\rho$.

The motion of the beam consists of three phases as follows.

(i) *Loaded phase, LBM2.* During this phase, $P(t) = P_m$ so that by repeated integration

of eqn (28) and use of the initial conditions we obtain

$$\dot{w}_p = \frac{P_m t}{m} \tag{30}$$

$$w_p = \frac{P_m t^2}{2m}. \tag{31}$$

Owing to the continuity of displacement and velocity at the hinge section, we can introduce eqns (30) and (31) into eqn (29) which yields a first order ordinary differential equation for $\rho(t)$ whose solution can be written as

$$L - \rho = L/\sqrt{(3/p)} \left[1 + \frac{1}{5} \left(\frac{P_m}{mh} \right)^2 t^4 \right]^{1/2}. \tag{32}$$

Equation (32) gives the instantaneous location of the plastic hinge in the interval $0 < \rho(t) < L$ and is valid for $t \leqslant \tau$. The initial position of the hinge is $\rho(0) = L[1 - \sqrt{(3/p)}]$ as was also obtained from infinitesimal bending theory[8, 14]. Equation (32) indicates that during the period of load application the plastic hinges move towards the centre.

The beam will not come to rest in this phase of motion since the central portion is always accelerating. The motion continues until:

(a) the deflections become large enough to initiate the string response at $t = t_s$,
(b) t reaches τ when the load is removed and the unloaded phase of motion begins, or
(c) the hinges reach the centre at $t = T$.

Case (a) can be analyzed in the manner described in Section 2.6. The analysis of case (c), which is essentially the same as that employed for the low load case, follows the various branches given in Fig. 2(a). Fortunately, this case only occurs for pressures, p, that are slightly greater than 3 and its analysis can be omitted with very little loss. Case (b) will be studied in the following.

(ii) *Unloaded phase, UBM2.* The motion in this phase is governed by eqns (28) and (29) with $P(t) = 0$. Thus

$$\ddot{w}_p = 0, \qquad 0 \leqslant x \leqslant \rho(t) \tag{33}$$

$$M_0 \left(1 + \frac{4}{h^2} w_p^2 \right) = -\tfrac{1}{3} m \ddot{w}_p \rho(L - \rho), \qquad \rho(t) \leqslant x \leqslant L. \tag{34}$$

It may be shown, using eqns (33) and (34) and matching the conditions at $t = \tau$ with those at the end of the loaded phase, that

$$[L - \rho]^2 = \frac{6M_0}{I} \left\{ t + \frac{4}{3} \left(\frac{I}{mh} \right)^2 (t - \tau/2)^3 + \frac{1}{30} \left(\frac{I}{mh} \right)^2 \tau^3 \right\}. \tag{35}$$

Equation (35) gives the hinge location in this phase. Since the central region moves with a constant velocity according to eqn (33), the beam cannot stop during this phase. However, one of the following two cases can occur.

(a) The width of the central flat region continues to shrink until at time $t = T$ the plastic hinges on either side of the midspan coalesce into a single hinge at the centre, i.e. $\rho(T) = 0$. Thereafter the third phase of motion ensues and the beam deforms in accordance with mechanism 1. It is in the latter phase that the final deformation can be reached for small deflections.

(b) The deflections become sufficiently large to initiate the string mode at which point $w_\rho(t_s) = h/2$.

The former case will be treated in the following.

(iii) *Unloaded phase, UBM*1. Since the deformation in this phase occurs by mechanism 1, the beam motion is governed by eqn (11) with $P(t) = 0$. Matching the conditions at $t = T$ with those at the end of the loaded phase, and setting $\dot{w}_0(t_f) = 0$, it can be shown that the final central deflection δ_f corresponding to point (K) of Fig. 2(b) is given by

$$\frac{\delta_f}{h} + \frac{4}{3}\left(\frac{\delta_f}{h}\right)^3 = \frac{I^2}{3mhP_0} + \frac{4}{3}\left(\frac{I}{mh}\right)^3 (T-\tau/2)^3 + \left(\frac{I}{mh}\right)(T-\tau/2). \tag{36}$$

Now by definition, $p(T) = 0$ and eqn (35) yields the following equation for the determination of T

$$T + \frac{4}{3}\left(\frac{I}{mh}\right)^2 (T-\tau/2)^3 = \frac{I}{3P_0} - \frac{1}{30}\left(\frac{I}{mh}\right)^2 \tau^3. \tag{37}$$

If eqn (37) is used to eliminate T from eqn (36), then we can write an expression for δ_f in terms of β and p as

$$\frac{\delta_f}{h} + \frac{4}{3}\left(\frac{\delta_f}{h}\right)^3 = \frac{2}{3}\beta - \frac{1}{2}(\beta/p) - \frac{1}{30}(\beta/p)^3. \tag{38}$$

If during this third phase of motion the central deflection reaches $h/2$, the beam goes into the string mode before it stops moving.

It is interesting to note that the formula derived by Symonds and Mentel[9] for the special case of impulsive loading can be recovered from eqn (38) by taking the limit $p \rightarrow \infty$. This is

$$\frac{\delta_f}{h} + \frac{4}{3}\left(\frac{\delta_f}{h}\right)^3 = \frac{2}{3}\beta_0 = \frac{2}{3}\frac{I_0^2}{mhP_0} \tag{39}$$

where I_0 is the ideal impulse corresponding to a load of infinite magnitude and zero duration.

2.6. *String mode*

The initial conditions for the loaded string mode response come from the beam mechanisms when the deflection reaches $h/2$. In the case of mechanism 1 which has straight sections connected to a central hinge, the initial deflection shape is quite different from the final string shape which is sinusoidal. However, Symonds and Jones[17] suggest that the initial deflected shape is not critical. Furthermore mechanism 1 is known to be an approximation to a smoother deflection shape. Hence we assume that the initial displacement is adequately represented by a half sine wave with amplitude $h/2$. The initial velocity distribution is also assumed to be sinusoidal with amplitude V_0 determined such that the kinetic energy matches that in the appropriate beam mechanism.

The initial conditions for the unloaded string mode (USM) can come from either the beam mechanism or the loaded string mode. In either case, their distributions are assumed to be sinusoidal with the initial amplitudes as described above.

The initial velocity amplitude is determined from

$$V_0 = \left[\frac{2}{L}\int_0^L \dot{w}^2(x, t_s)\,\mathrm{d}x\right]^{1/2}. \tag{40}$$

The equation governing the motion of the string can be obtained from eqn (1) after setting $M(x, t) = 0$ and $N = N_0$. Thus

$$\ddot{w}(x, t) = c^2 w''(x, t) + P(t); \qquad t \geqslant t_s \tag{41}$$

where

$$c = \sqrt{(N_0/m)} \tag{42}$$

has the form of a wave speed.

(i) *Loaded string mode, LSM*. In the case that the string comes to rest while the load is still on, it is easy to show that the permanent central displacement is given by

$$\frac{\delta_f}{h} = \sqrt{(A^2 + B^2)} + \left(\frac{2}{\pi}\right)^3 p \tag{43}$$

where

$$A = \frac{2L}{\pi ch} V_0 = \begin{cases} \dfrac{1}{\pi} [\tfrac{2}{3}(3p - 4)]^{1/2}, & \tfrac{4}{3} \leqslant p < 3 \tag{44a} \\[2ex] \dfrac{2}{\pi} [p - 2\sqrt{(2p/5)}]^{1/2}, & p > 3 \tag{44b} \end{cases}$$

and

$$B = \frac{1}{2} - \left(\frac{2}{\pi}\right)^3 p. \tag{45}$$

(ii) *Unloaded string mode, USM*. In this case, the string mode motion continues after the load is removed and the permanent central displacement becomes

$$\frac{\delta_f}{h} = \sqrt{(C^2 + D^2)} \tag{46}$$

where C and D are found by matching conditions at $t = \tau$. Thus

$$C = A \cos \mu - B \sin \mu \tag{47}$$

$$D = A \sin \mu + B \cos \mu + \left(\frac{2}{\pi}\right)^3 p \tag{48}$$

where μ is defined as

$$\mu = \frac{\pi c}{2L}(\tau - t_s) = \begin{cases} \dfrac{\pi}{\sqrt{2}} \left\{ \dfrac{\sqrt{\beta}}{p} - \left[\dfrac{1}{3(p-1)}\right]^{1/4} [K - F(1/\sqrt{2}, \phi_s)] \right\}, & \text{for } \tfrac{4}{3} \leqslant p < 3 \tag{49a} \\[3ex] \dfrac{\pi}{\sqrt{2}} \left[\dfrac{\sqrt{\beta}}{p} - \dfrac{1}{\sqrt{p}} \right], & \text{for } p > 3. \tag{49b} \end{cases}$$

For those combinations of β and p which result in $\mu \geqslant \mu_c$, where

$$\mu_c = \begin{cases} \tan^{-1}(A/B) & \text{for } p < \pi^3/16 \tag{50a} \\ \tan^{-1}(A/B) + \pi & \text{for } p > \pi^3/16 \tag{50b} \end{cases}$$

it can be shown that the final deflection of the string is attained during the load application and its magnitude is determined by eqn (43).

When the string stage is reached in the unloaded state of the beam, the maximum permanent deflection of the string is given by

$$\frac{\delta_f}{h} = \left\{ \frac{1}{4} + \frac{4L^2}{\pi^2 c^2 h^2} V_0^2 \right\}^{1/2} \tag{51}$$

which can be expressed in terms of β and p after V_0 is determined from eqn (40).

3. RESPONSE RESULTS

After carrying out all the solution steps outlined in the preceding section, we obtain the final equations for the permanent deflection. These are summarized in detail in the Appendix for both simply supported and clamped boundary conditions. The circled letters refer to the corresponding lettered points in Figs 2(a) and (b) and indicate the applicable branch of the solution process. Also shown are the parameter regimes of validity for each particular formula. Some of the deflection responses are shown graphically and discussed in the following.

3.1. *Low load*

The final central deflection δ_f/h is shown plotted in Fig. 4 against the impulse parameter β for a few representative values of the nondimensional pressure p within the low range, $1 < p \leqslant 3$. To the left of the cross-hatched line the duration of load is small enough so that the load is removed before the beam comes to rest, and so the response depends on the impulse. To the right of the line the load is still on, and could remain on with no further deformation, and so the final deflection is independent of the impulse.
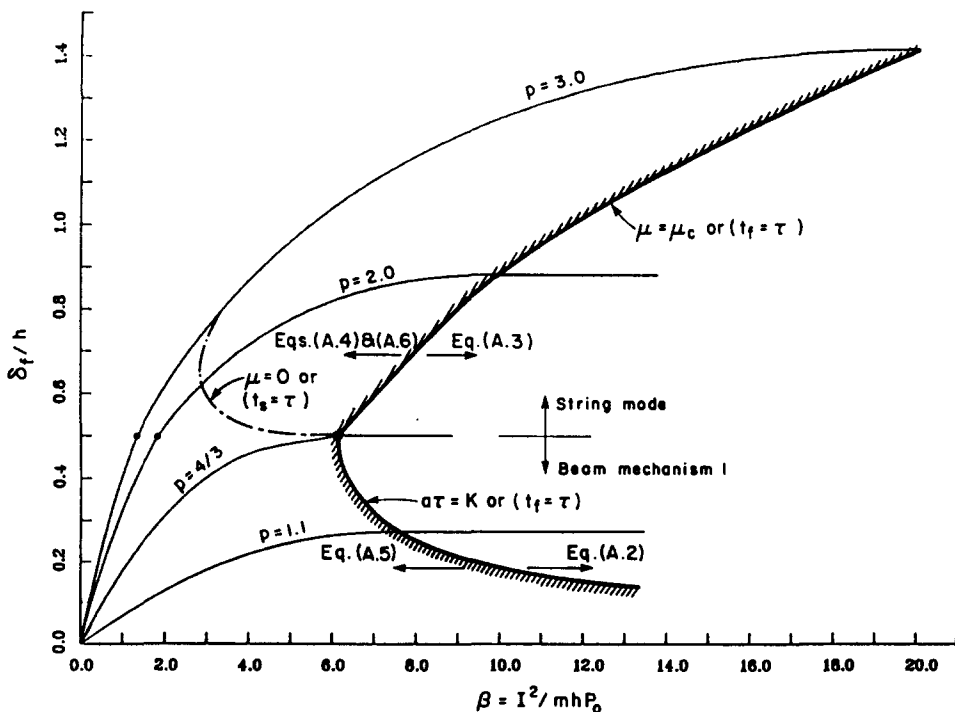

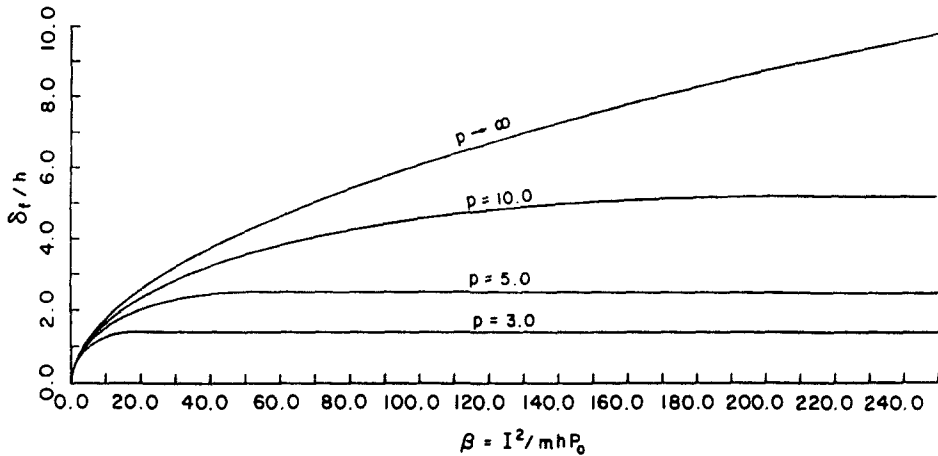Fig. 4. Simply supported beam deflection curves for low load.

Fig. 5. Simply supported beam deflection curves for high load.

3.2. *High load*

The corresponding curves for $p \geqslant 3$ are shown in Fig. 5. In this range of pressures the results show that for short duration loads the response is sensitive to the impulse only, but that for long duration loads the pressure is the important parameter.

A comparison of the results of this analysis with those of Symonds and Mentel[9] and with experimental results[10, 17, 18], for the case of pure impulsive loads on a clamped beam is shown in Fig. 6. Also shown is the pure bending response. It is seen that the present results compare favourably with the experimental values. The experimental results are all for steel samples which do show some strain rate effects, and so it is to be expected that the analytical results would be above the experimental ones.

4. ISODAMAGE CURVES

4.1. *Construction of isodamage curves*

A useful way of representing the response of a structure is to establish the appropriate "isoresponse" or "isodamage" curves. These are the loci of combinations of pressure and
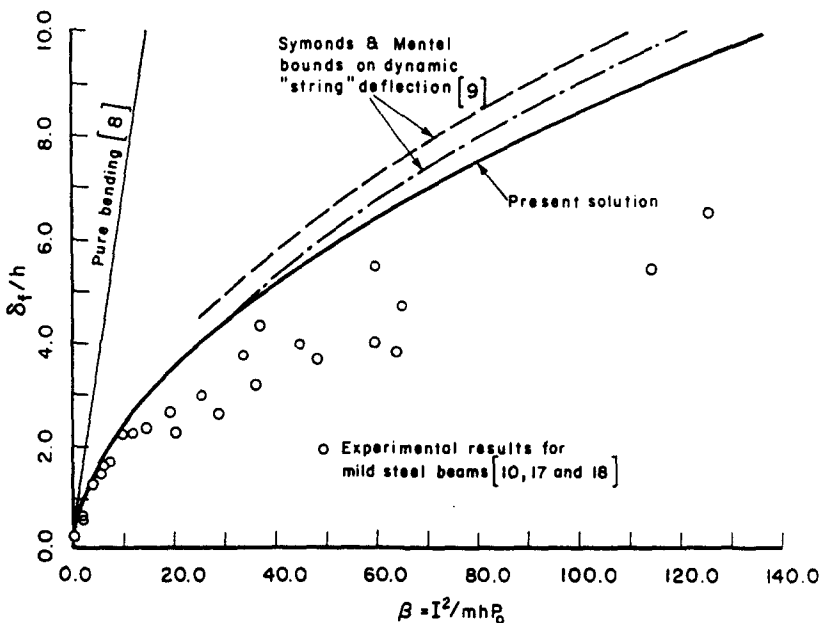

Fig. 6. Comparison of experimental and theoretical deflection of impulsively loaded clamped beams.

impulse that produce the same response, in this case the maximum displacement of the structure[19]. In this section, we construct the simply supported beam isodamage curves for two distinct levels of damage typified by small damage ($\delta_f/h \leqslant 0.5$) and severe damage ($\delta_f/h \geqslant 0.5$). Whenever reference is made to an equation in the tables, the simply supported formula is implied.

4.1.1. *Small damage* ($\delta_f/h \leqslant 0.5$). Keeping δ_f/h as a fixed quantity, the following equation for β results from eqns (23) and (38).

$$\beta = \frac{p^2}{\sqrt{(3(p-1))}}[F(1/\sqrt{2}, \phi)]^2 \qquad \text{for} \quad 1 < p \leqslant 3 \tag{52}$$

where $\phi = \phi(p, \delta_f/h)$ is given by

$$\phi = \sin^{-1}\sqrt{\{\gamma/(1+\gamma/2)\}} \tag{53}$$

with

$$\gamma = 4\left[\frac{\delta_f}{h} + \frac{4}{3}\left(\frac{\delta_f}{h}\right)^3\right]\Big/[p\sqrt{(3(p-1))}]. \tag{54}$$

For $p \geqslant 3$ the impulse parameter β is given by the smallest positive real root of the polynomial equation

$$\frac{1}{30}(\beta/p)^3 + (\beta/p)\left[\frac{1}{2} - \frac{2}{3}p\right] + \frac{\delta_f}{h} + \frac{4}{3}\left(\frac{\delta_f}{h}\right)^3 = 0 \qquad \text{for} \quad p \geqslant 3. \tag{55}$$

Equations (52) and (55) give the p–β combinations that produce the same final deflection δ_f/h. As $\beta \rightarrow \infty$, the response can be characterized by a single parameter, namely the pressure parameter p_c given by

$$p_c = 1 + \frac{4}{3}\left(\frac{\delta_f}{h}\right)^2; \qquad 1 \leqslant p_c \leqslant \frac{4}{3} \tag{56}$$

which follows from eqn (20). The value of the impulse parameter β_c beyond which the dynamic pulse can be characterized by a step load, is given by the root of equation $a\tau = K$, or

$$\beta_c = \frac{p_c^2 K^2}{\sqrt{(3(p_c - 1))}} = \frac{K^2}{2}\left[1 + \frac{4}{3}\left(\frac{\delta_f}{h}\right)^2\right]^2 \Big/ \frac{\delta_f}{h}. \tag{57}$$

The upper part of the isoresponse curves are asymptotic to an impulse parameter β_0 given by eqn (39) as

$$\beta_0 = \frac{3}{2}\left[\left(\frac{\delta_f}{h}\right) + \frac{4}{3}\left(\frac{\delta_f}{h}\right)^3\right]. \tag{58}$$

In the intermediate dynamic loading realm (knee of the curve), both parameters β and p influence the permanent deflections.

4.1.2. *Severe damage* ($\delta_f/h \geqslant 0.5$). It may be shown that for $1 < p \leqslant 3$, $\delta_f/h < 1.42$. Hence we construct the pressure–impulse curves separately for damage above and below this level.

(i) $0.5 < \delta_f/h < 1.42$: the value of the pressure parameter p_c in this case is given by eqn (A.3) as

$$p_c = \frac{\left(\dfrac{\delta_f}{h}\right) - \dfrac{1}{4} + \dfrac{2}{3}\left(\dfrac{2}{\pi}\right)^2}{\dfrac{1}{2}\left(\dfrac{2}{\pi}\right)^2 - \left(\dfrac{2}{\pi}\right)^3 + 2\left(\dfrac{2}{\pi}\right)^3\dfrac{\delta_f}{h}}, \qquad \tfrac{4}{3} \leqslant p_c \leqslant 3. \tag{59}$$

The corresponding value of the impulse parameter β_c required to achieve the same central deflection δ_f/h can be obtained from eqn (49a) as

$$\beta_c = p_c^2\left\{\frac{\sqrt{2}}{\pi}\mu_c + \left[\frac{1}{3(p_c-1)}\right]^{1/4}[K - F(1/\sqrt{2}, \phi_s)]\right\} \tag{60}$$

where μ_c is defined by eqns (50a, b) with p replaced by p_c. For $\beta > \beta_c$, it is sufficient to represent the load intensity by p_c. As pressure is increased from p_c to $p = 3$, the pressure–impulse relationship can be described by

$$\beta = p^2\left\{\frac{\sqrt{2}}{\pi}\mu + \left[\frac{1}{3(p-1)}\right]^{1/4}[K - F(1/\sqrt{2}, \phi_s)]\right\} \tag{61}$$

for $p_c \leqslant p \leqslant 3$ and $\mu \geqslant 0$, where

$$\mu = \sin^{-1}\left\{\frac{R}{\sqrt{(A^2+B^2)}}\right\} - \sin^{-1}\left\{\frac{B}{\sqrt{(A^2+B^2)}}\right\}. \tag{62}$$

In the above the inverse sine is an angle between $-\pi/2$ and $\pi/2$ with A and B given by eqns (44a) and (45), respectively, and R defined as

$$R = \frac{\pi^3}{16p}\left[\left(\frac{\delta_f}{h}\right)^2 - (A^2+B^2) - \left(\frac{2}{\pi}\right)^6 p^2\right]. \tag{63}$$

If p is increased to a level that renders the quantity μ negative, then eqn (A.6) prevails and the β–p relationship becomes

$$\beta = \frac{p^2}{\sqrt{(3(p-1))}}[F(1/\sqrt{2}, \phi)]^2 \quad \text{for} \quad p_c \leqslant p \leqslant 3 \quad \text{and} \quad \mu \leqslant 0 \tag{64}$$

where ϕ is given by eqn (53) in which

$$\gamma = \left\{\pi^2\left[\left(\frac{\delta_f}{h}\right)^2 - \frac{1}{4}\right] + \frac{8}{3}\right\}\Big/[p\sqrt{(3(p-1))}]. \tag{65}$$

The remaining part of the p–β curve beyond $p = 3$ comes from the string mode. Using eqns (A.8), (A.9) and (A.11) leads to

$$\beta = p^2\left[\frac{\sqrt{2}}{\pi}\mu + \frac{1}{\sqrt{p}}\right] \tag{66}$$

for $p \geqslant 3$ and for $\mu \geqslant 0$, where μ is again given by eqn (62) but now the quantity a is defined by eqn (44b).

If μ becomes negative for high pressure, two different cases arise according to whether the plastic hinges are within the half-span (i.e. $0 < \rho \leqslant L$) or at the midspan (i.e. $\rho = 0$) prior to the onset of the string mode. The relevant equations become

$$\frac{2}{45p^3}\beta^4 + \left(\frac{2}{3p} - 1\right)\beta^2 + \left[\frac{8}{9} + \frac{\pi^2}{2}\left(\left(\frac{\delta_f}{h}\right)^2 - \frac{1}{4}\right)\right]\beta - \frac{\pi^4}{16}\left[\left(\frac{\delta_f}{h}\right)^2 - \frac{1}{4}\right]^2 = 0 \qquad (67)$$

for $p \geqslant 3, p \geqslant \beta$ and $2 + \frac{3}{2}(\beta/p) + \frac{1}{10}(\beta/p)^3 \leqslant \beta$

and

$$\frac{1}{30p^3}\beta^3 + \left(\frac{1}{2p} - \frac{2}{3}\right)\beta + \frac{2}{3} + \frac{\pi^2}{4}\left[\left(\frac{\delta_f}{h}\right)^2 - \frac{1}{4}\right] = 0 \qquad (68)$$

for $p \geqslant 3, p \geqslant \beta$ and $2 + \frac{3}{2}(\beta/p) + \frac{1}{10}(\beta/p)^3 \geqslant \beta$.

For very high loads as $p \to \infty$, we obtain from eqns (67) and (68)

$$\beta_0 = 1 + \frac{3\pi^2}{8}\left[\left(\frac{\delta_f}{h}\right)^2 - \frac{1}{4}\right] \qquad (69)$$

provided $\beta_0 \leqslant 2$ or $\dfrac{\delta_f}{h} \leqslant 0.72$ and

$$\beta_0 = \tfrac{1}{2}[\xi + \sqrt{(\xi^2 - 4\zeta)}] \qquad (70)$$

for $0.72 \leqslant \dfrac{\delta_f}{h} \leqslant 1.42$, where

$$\xi = \frac{8}{9} + \frac{\pi^2}{2}\left[\left(\frac{\delta_f}{h}\right)^2 - \frac{1}{4}\right] \qquad (71)$$

$$\zeta = \frac{\pi^4}{16}\left[\left(\frac{\delta_f}{h}\right)^2 - \frac{1}{4}\right]^2. \qquad (72)$$

Equations (69) and (70) define the location of the vertical asymptotes in the p–β space and represent the value of the ideal impulse which produces the same damage δ_f/h as the rectangular pulses of finite durations.

(ii) $\delta_f/h > 1.42$: for this case, using eqn (A.7), the pressure p_c is given by

$$p_c = \frac{q}{s} + \left[\left(\frac{q}{s}\right)^2 - \frac{1}{s}\left\{\left(\frac{\delta_f}{h}\right)^2 - \frac{1}{4}\right\}\right]^{1/2} \qquad (73)$$

where

$$s = \left[\left(\frac{2}{\pi}\right)^2 - \left(\frac{2}{\pi}\right)^3 + 2\left(\frac{2}{\pi}\right)^3\frac{\delta_f}{h}\right]^2 \qquad (74)$$

and

$$q = \sqrt{s}\left[\left(\frac{\delta_f}{h}\right)^2 - \frac{1}{4}\right] + \frac{4}{5}\left(\frac{2}{\pi}\right)^4. \qquad (75)$$
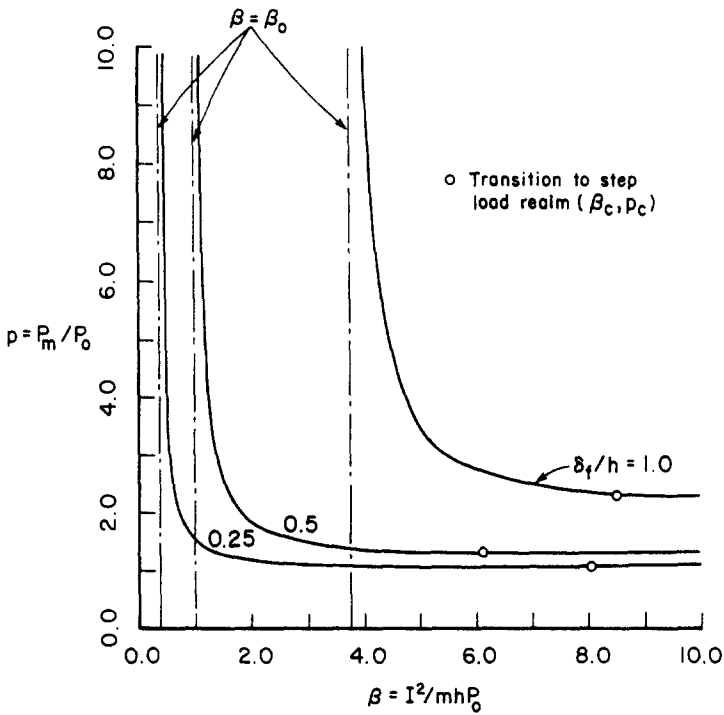
Fig. 7. Simply supported beam isodamage curves for low damage.

The impulse parameter β_c beyond which the response depends primarily on the pressure magnitude is given by eqn (66) with p replaced by p_c defined above. The points with coordinates (β, p) that describe the dynamic and impulsive parts of the isoresponse curve can once again be obtained from eqns (67)–(69).

4.2. Results

The results of the previous section are shown plotted in Figs 7 and 8 for the simply supported beam. These are true isodamage curves showing the relationship which must exist between pressure and impulse in order to produce a given level of damage, the
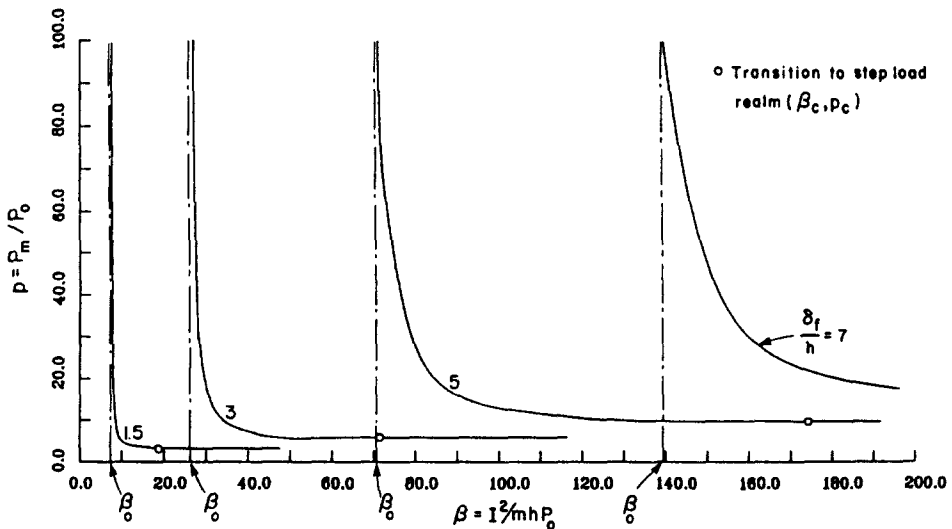

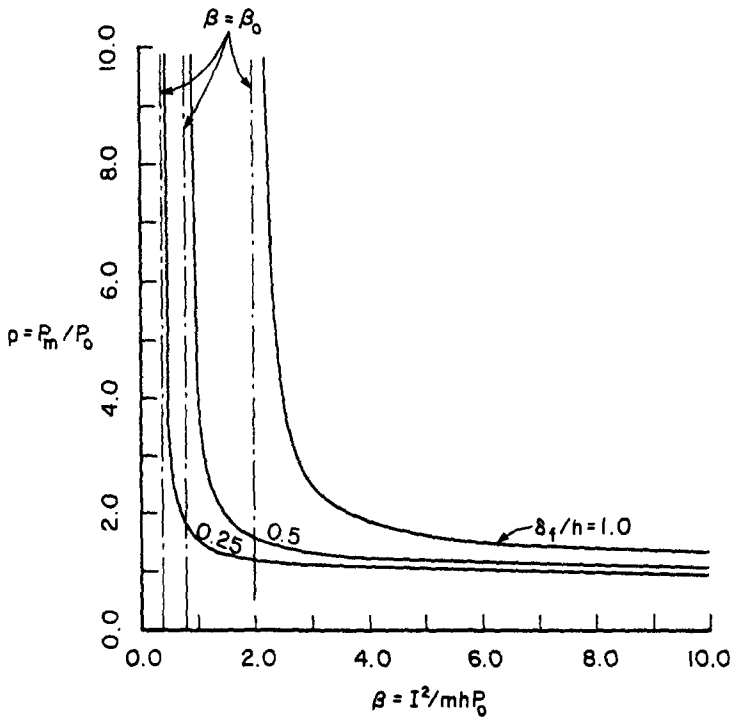Fig. 8. Simply supported beam isodamage curves for severe damage.

Fig. 9. Clamped beam isodamage curves for low damage.

permanent deflection in this case. Figure 7 shows the low damage case for $\delta_f/h = 0.25, 0.5$ and 1.0, and Fig. 8, the severe damage case for $\delta_f/h = 1.5, 3, 5$ and 7.

The corresponding curves for the clamped beam are shown in Figs 9 and 10. The equations for these curves were obtained from the results given in the Appendix following the same procedures as in Section 4.1 for the simply supported beam. The static collapse pressure P_0 used in these figures was the appropriate clamped beam value (i.e. two times the simply supported value). Note that the scales of Figs 7 and 9 are the same to facilitate comparison whereas those of Figs 8 and 10 are not.

The vertical asymptotes for the limiting case of impulsive loading are shown dashed
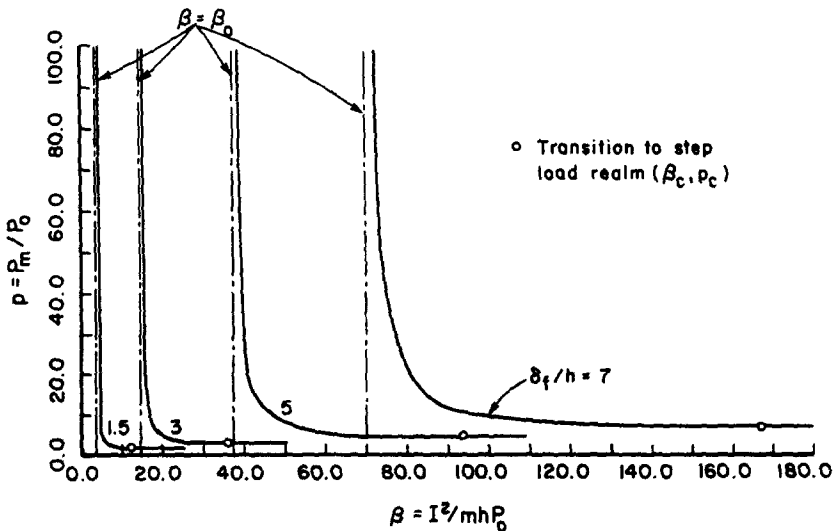

Fig. 10. Clamped beam isodamage curves for severe damage.

in all the figures and designated by $\beta = \beta_0$. Also shown by small circles are the points of transition to the step load realm, i.e. points where the beam comes to rest just as the load is removed.

The curves shown in Figs 7–10 indicate that the pressure and impulse must increase rapidly in a nonlinear manner to produce higher levels of damage. If the curves for the simply supported and clamped beam are superimposed, they unfortunately do not fall together. However if they are replotted with dimensional pressure–impulse scales, they lie quite close together with the clamped curves slightly to the right and above the simply supported ones (because the clamped beam requires slightly more energy for the same damage). The isodamage curves shown here are believed to be the first ever published for the fully nonlinear beam response.

5. CONCLUSIONS

An approximate analytical procedure, which includes the effects of finite geometry changes, has been developed herein to predict the response of axially constrained rigid-plastic beams subjected to dynamic pulses of severe intensity. A closed form solution has been derived for the simplest case, that of a rectangular beam acted on by a rectangular pressure pulse of arbitrary magnitude and duration. The permanent central deflection was found to depend strongly on both the pressure and the impulse.

It is encouraging to note that the results for the special case of a fully clamped beam subjected to impulsive loading agree reasonably well with the corresponding experimental values. The theoretical predictions for the response of beams to dynamic loads of finite durations cannot be compared with experimental results since (to the authors' knowledge) no test data seem to have been reported for this case. Moreover, due to the lack of relevant uniqueness or bounding theorems, it is impossible to assess whether the present predictions are smaller or larger than the exact solution. An assessment of the validity of the various approximations made in the theory outlined herein must await information from experiments and/or numerical elasto-plastic solutions. Nevertheless until such supporting confirmation of the theory are obtained the predictions obtained here are believed to be sufficiently accurate for preliminary design work. It should be noted, however, that the present rigid-plastic results will be unconservative for low load levels with pulse durations of the order of the elastic period of the structure. See [20] for estimates of the potential error.

The final results presented as structural isodamage curves are particularly useful in predicting the characteristics of the rectangular pulse required to cause a specified permanent deformation of the beam. These isodamage plots provide a simple presentation of the theoretical results and are extremely important in planning experiments.

It appears quite clear from the present study that geometry changes have a considerable influence on the dynamic behaviour of beams even for small deflections and therefore they should be retained in any dynamic analysis of beams with axial restraints.

REFERENCES

1. N. Jones, A literature review of the dynamic plastic behaviour of structures. *Shock and Vibration Digest*, Vol. 7, August 1975, pp. 89–105.
2. N. Jones, Recent progress in the dynamic plastic behaviour of structures, Parts 1 and 2. *Shock and Vibration Digest*, Vol. 10, September 1978, pp. 21–33 and October 1978, pp. 13–19.
3. N. Jones, Recent progress in the dynamic plastic behaviour of structures. *Shock and Vibration Digest*, Part 3, Vol. 13, October 1981, pp. 3–16.
4. W. E. Baker, Approximate techniques for plastic deformation of structures under impulsve loading, III. *Shock and Vibration Digest*, Vol. 14, November 1982, pp. 3–11.
5. P. S. Symonds, Survey of methods of analysis for plastic deformation of structures under dynamic loadings. Brown University, Report BU/NSRDC/1-67 (1967).
6. J. Ari-Gur, D. L. Anderson and M. D. Olson, Air-blast response of beams and plates. Structural Research Series, Report No. 30, Dept. of Civil Engineering, University of British Columbia, Vancouver, Canada, June

(1983). See also paper in *Procs. 2nd Int. Conf. on Recent Advances in Struct. Mech.*, University of Southampton, U.K. (1984).

7. E. H. Lee and P. S. Symonds, Large plastic deformations of beams under transverse impact. *J. Appl. Mech. Trans. ASME* **74**, 308 (1952).
8. P. S. Symonds, Large plastic deformations of beams under blast type loading. *Proc. of the 2nd U.S. National Congress of Applied Mechanics, ASME*, pp. 505–515 (1954).
9. P. S. Symonds and T. J. Mentel, Impulsive loading of plastic beams with axial constraints. *J. Mech. Phys. Solids* **6**, 186 (1958).
10. J. S. Humphreys, Plastic deformation of impulsively loaded straight clamped beams. *J. Appl. Mech. Trans. ASME* **22**, 7 (1965).
11. T. Nonaka, Some interaction effects in a problem of plastic beam dynamics, Parts I–III. *J. Appl. Mech. Trans. ASME* **34**, 623 (1967).
12. N. Jones, Influence of strain-hardening and strain-rate sensitivity on the permanent deformation of impulsively loaded rigid-plastic beams. *Int. J. Mech. Sci.* **9**, 777 (1967).
13. N. Jones, A theoretical study of the dynamic plastic behaviour of beams and plates with finite-deflections. *Int. J. Solids Structures* **7**, 1007 (1971).
14. D. Krajcinovic, Dynamic response of rigid-plastic beams—general case of loading. *J. Struct. Mech.* **3**, 439 (1975).
15. R. Vaziri, Finite deflection dynamic analysis of rigid-plastic beams. Structural Research Series, Report No. 31, Dept. of Civil Engineering, University of British Columbia, Vancouver, Canada, May (1985).
16. E. T. Onat and W. Prager, Limit analysis of arches. *J. Mech. Phys. Solids* **1**, 77 (1953).
17. P. S. Symonds and N. Jones, Impulsive loading of fully clamped beams with finite plastic deflections and strain-rate sensitivity. *Int. J. Mech. Sci.* **14**, 49 (1972).
18. N. Jones, R. N. Griffin and R. E. Van Duzer, An experimental study into the dynamic plastic behaviour of wide beams and rectangular plates. *Int. J. Mech. Sci.* **13**, 721 (1971).
19. G. Abrahamson and H. E. Lindberg, Peak load-impulse characterization of critical pulse loads in structural dynamics. *Proceedings of a Symposium held at Stanford University, California* (Edited by G. Herrman and N. Perrone), pp. 31–53. June (1971).
20. P. S. Symonds, Elastic–plastic deflections due to pulse loading. *Proceedings of the Second Speciality Conference on Dynamic Response of Structures: Experimentation, Observation, Prediction and Control* (Edited by G. Hart), pp. 887–901. New York, ASCE (1980).

APPENDIX

Summary of results, including beams with clamped ends

The results obtained for simply supported beams can be made to apply to clamped beams by merely replacing the critical moment M by $2M$ whenever it occurs in each equation (this also includes the replacement of M_0 by $2M_0$) (see Refs [8, 9]). In accordance with the above modification the flow rule [eqn (4)] takes the form

$$\frac{N}{N_0} = \frac{N_0 w_0}{4M_0} = \frac{w_0}{h} \leqslant 1. \tag{A.1}$$

It can be seen that the beam solution is now valid for central deflections less than h, the full depth of the beam, as opposed to the half-depth for the simply supported case. The formulas for the permanent central deflection of simply supported and fully clamped beams are both presented in the following tables. Note that the circled letters A, B, etc., refer to the solution branch points shown in Figs 2(a) and (b).

Table A.1. Comparison of various parameters used in the analysis of simply supported and clamped beams

Parameter	Simply supported beam	Clamped beam
P_0	$2M_0/L^2$	$4M_0/L^2$
ϕ_s	$\cos^{-1}\left[\dfrac{1}{3(p-1)}\right]^{1/4}$	$\cos^{-1}\left[\dfrac{1}{3(p-1)}\right]^{1/4}$
$a\tau$	$\sqrt{\beta}[3(p-1)]^{1/4}/p$	$\sqrt{(\beta/2)}\,[3(p-1)]^{1/4}/p$
$L-\rho(t_s)$	$L\left[2/\beta+3/2p+\dfrac{1}{10}(\beta^2/p^3)\right]^{1/2}$	$L\left[4/\beta+3/2p+\dfrac{1}{40}(\beta^2/p^3)\right]^{1/2}$
μ $\begin{cases} 1 < p \leqslant 3 \\[6pt] p \geqslant 3 \end{cases}$	$\dfrac{\pi}{\sqrt{2}}\left\{\dfrac{\sqrt{\beta}}{p}-\left[\dfrac{1}{3(p-1)}\right]^{1/4}[K-F(1/\sqrt{2},\phi_s)]\right\}$ $\dfrac{\pi}{\sqrt{2}}\left\{\dfrac{\sqrt{\beta}}{p}-\dfrac{1}{\sqrt{p}}\right\}$	$\dfrac{\pi}{\sqrt{2}}\left\{\dfrac{\sqrt{(\beta/2)}}{p}-\left[\dfrac{1}{3(p-1)}\right]^{1/4}[K-F(1/\sqrt{2},\phi_s)]\right\}$ $\dfrac{\pi}{\sqrt{2}}\left\{\dfrac{\sqrt{(\beta/2)}}{p}-\dfrac{1}{\sqrt{p}}\right\}$
μ_r	eqns (50a) and (50b)	eqns (50a) and (50b)

Table A.2. Theoretical prediction of final central deflection of simply supported and clamped beams: low load $1 < p \leqslant 3$

Terminal points in Fig. 2(a)		Simply supported beam	Clamped beam	Eqn
Ⓐ	$1 \leqslant p \leqslant 4/3$ $a\tau > K$	$\dfrac{\delta_f}{h} = \dfrac{\sqrt{3}}{2}[p-1]^{1/2}$	$\dfrac{\delta_f}{h} = \sqrt{3}[p-1]^{1/2}$	(A.2)
Ⓑ	$4/3 \leqslant p \leqslant 3$ $\mu > \mu_c$	$\dfrac{\delta_f}{h} = \sqrt{(A^2+B^2)} + \left(\dfrac{2}{\pi}\right)^3 p$	$\dfrac{\delta_f}{h} = 2\sqrt{(A^2+B^2)} + 2\left(\dfrac{2}{\pi}\right)^3 p$	(A.3)
Ⓒ	$4/3 \leqslant p \leqslant 3$ $0 < \mu < \mu_c$	$\dfrac{\delta_f}{h} = \sqrt{(C^2+D^2)}$	$\dfrac{\delta_f}{h} = 2\sqrt{(C^2+D^2)}$	(A.4)
Ⓓ	$1 < p \leqslant 4/3$ $a\tau < K$	$\dfrac{\delta_f}{h} + \dfrac{4}{3}\left(\dfrac{\delta_f}{h}\right)^3 = \dfrac{2}{3}(\Lambda^2+1)$	$\dfrac{\delta_f}{h} + \dfrac{1}{3}\left(\dfrac{\delta_f}{h}\right)^3 = \dfrac{4}{3}(\Lambda^2+1)$	(A.5)
Ⓔ	$4/3 \leqslant p \leqslant 3$ $\mu < 0$	$\dfrac{\delta_f}{h} = \left[\dfrac{1}{4} + \dfrac{8}{3\pi^2}\Lambda^2\right]^{1/2}$	$\dfrac{\delta_f}{h} = \left[1 + \dfrac{32}{3\pi^2}\Lambda^2\right]^{1/2}$	(A.6)

A, B, C and *D* are given by eqns (44a), (45), (47) and (48).

$$\Lambda = \left[\frac{\sqrt{3}}{8}p\sqrt{(3(p-1))}sd^2(a\tau) - 1\right]^{1/2}.$$

Table A.3. Theoretical prediction of final central deflection of simply supported and clamped beams: high load $p \geqslant 3$

Terminal points in Fig. 2(b)		Simply supported beam	Clamped beam	Eqn
Ⓕ		No permanent deformation	No permanent deformation	
Ⓖ	$\mu > \mu_c$	$\dfrac{\delta_f}{h} = \sqrt{(A^2+B^2)} + \left(\dfrac{2}{\pi}\right)^3 p$	$\dfrac{\delta_f}{h} = 2\sqrt{(A^2+B^2)} + 2\left(\dfrac{2}{\pi}\right)^3 p$	(A.7)
Ⓗ	$0 < \mu < \mu_c$	$\dfrac{\delta_f}{h} = \sqrt{(C^2+D^2)}$	$\dfrac{\delta_f}{h} = 2\sqrt{(C^2+D^2)}$	(A.8)
Ⓘ		No permanent deformation	No permanent deformation	
Ⓙ	$\mu < 0$ $\rho(t_s) \geqslant 0$	$\dfrac{\delta_f}{h} = \left[\dfrac{1}{3}\left(\dfrac{2}{\pi}\right)^2 \beta\left[1 + 2\dfrac{\rho(t_s)}{L}\right] + \dfrac{1}{4}\right]^{1/2}$	$\dfrac{\delta_f}{h} = \left[\dfrac{2}{3}\left(\dfrac{2}{\pi}\right)^2 \beta\left[1 + 2\dfrac{\rho(t_s)}{L}\right] + 1\right]^{1/2}$	(A.9)
Ⓚ		$\dfrac{\delta_f}{h} + \dfrac{4}{3}\left(\dfrac{\delta_f}{h}\right)^3 = \dfrac{2}{3}\beta - \dfrac{1}{2}(\beta/p) - \dfrac{1}{30}(\beta/p)^3$	$\dfrac{\delta_f}{h} + \dfrac{1}{3}\left(\dfrac{\delta_f}{h}\right)^3 = \dfrac{2}{3}\beta - \dfrac{1}{2}(\beta/p) - \dfrac{1}{120}(\beta/p)^3$	(A.10)
Ⓛ	$\mu < 0$ $\rho(t_s) \leqslant 0$	$\dfrac{\delta_f}{h} = \left\{\left(\dfrac{2}{\pi}\right)^2\left[\dfrac{2}{3}(\beta-1) - \dfrac{1}{2}(\beta/p) - \dfrac{1}{30}(\beta/p)^3\right] + \dfrac{1}{4}\right\}^{1/2}$	$\dfrac{\delta_f}{h} = \left\{2\left(\dfrac{2}{\pi}\right)^2\left[\dfrac{2}{3}(\beta-2) - \dfrac{1}{2}(\beta/p) - \dfrac{1}{120}(\beta/p)^3\right] + 1\right\}^{1/2}$	(A.11)

A, B, C and *D* are given by eqns (44b), (45), (47) and (48).